Kinetics of Surface Enrichment of a Polymer in a Glass-Forming Molecular Liquid

Junguang Yu[1], Xin Yao[1], Chailu Que[2], Lian Huang[2], Ho-Wah Hui[2], Yuchuan Gong[2,3], Feng Qian[4], Lian Yu[1,5,*]

[1] School of Pharmacy, University of Wisconsin-Madison, Madison, WI, 53705, USA

[2] Drug Product Development, Bristol Myers Squibb, 556 Morris Avenue, Summit, NJ 07901, USA

[3] Small Molecule CMC, BeiGene (Beijing) Co., Ltd., Beijing 102206, China

[4] School of Pharmaceutical Sciences and Beijing Advanced Innovation Center for Structural Biology, Tsinghua University, Beijing 100084, China

[5] Department of Chemistry, University of Wisconsin-Madison, Madison, WI, 53705, USA

Abstract:

X-ray photoelectron spectroscopy (XPS) has been used to measure the surface concentration and the surface enrichment kinetics of a polymer in a glass-forming molecular liquid. As a model, the bulk-miscible system maltitol-polyvinylpyrrolidone (PVP) was studied. The PVP concentration is significantly higher at the liquid/vapor interface than in the bulk by up to a factor of 170 and the effect increases with its molecular weight. At a freshly created liquid/vapor interface, the concentration of PVP gradually increases from the bulk value at a rate controlled by bulk diffusion. The polymer diffusion coefficient obtained from the kinetics of surface enrichment agrees with that calculated from viscosity and the Stokes-Einstein equation. Our finding allows prediction of the rate at which the surface composition equilibrates in an amorphous material after milling, fracture, and a change of ambient temperature.

Keywords: Amorphous solid dispersion, surface concentration, surface enrichment kinetics, polymer, XPS

Corresponding Author

*E-mail: lian.yu@wisc.edu

Introduction

Amorphous (glassy) materials play an essential role in science and technology. An important property of glasses is compositional flexibility. While crystallization rejects impurities, glass formation often accommodates multiple components in a single phase.[1] This leads to optical transparency and continuous tuning of composition. An important multi-component glassy material is the drug-polymer Amorphous Solid Dispersion (ASD), which is increasingly used to enhance the solubility and bioavailability of poorly soluble drugs.[2] A typical ASD contains a drug, a polymer, and a surfactant[3] and can be produced by spray drying, hot melt extrusion, and other methods.[4]

Recent work has highlighted the importance of free surfaces in the fabrication and stability of glasses.[5] Crystal growth on the surface of a glass can be orders of magnitudes faster than that in the bulk, a consequence of the greater mobility of surface molecules.[6] Even in the interior of a glass, fast crystal growth can occur along cracks and through self-propagating micro-fractures.[7] Meanwhile, fast surface crystallization can be inhibited by an ultra-thin polymer coating.[8, 9] This coating, in essence, converts highly mobile surface molecules to less mobile bulk molecules. Besides stability, a polymer coating can improve wetting, dissolution, and other properties of an amorphous drug.[8] All these results underscore the importance of understanding the surface composition and dynamics in developing amorphous materials.

The surface composition of a multi-component amorphous material can be significantly different from its bulk composition.[10, 11,12,13] This is a consequence of component enrichment or deletion in the surface layer to reduce surface energy. The phenomenon is well known for the aqueous solutions of surfactants and has been observed in spray-dried milk[14] and drug formulations.[15, 16] Recently Yu et al. reported that common pharmaceutical surfactants can enrich at the surface of an amorphous drug, sometimes forming a nearly pure layer.[17] The surface segregation of components can potentially impact the stability, wetting, and dissolution of ASDs.

Although the thermodynamics of surface enrichment is reasonably well understood, less is known about its kinetics. For a solution, compositional equilibrium is established quickly at a liquid/vapor interface. For a glass-forming material, however, the timescale for compositional equilibration could be much longer, especially for slow-diffusing macromolecules. If a fresh surface is created in an amorphous solid by fracture or milling, how long will it take for the local concentration to evolve from the initial bulk value to the final surface value? ASDs prepared by melt extrusion are often milled and compacted during tableting, both processes potentially creating fresh surfaces. Conversely, if a polymer coating is applied to an amorphous solid, what is the rate at which the polymer migrates into the bulk? Answering these questions will help predict the stability of ASDs and the change of their performance over time.

In this study we investigate the kinetics of surface enrichment of a polymer in a glass-forming liquid. As a model the bulk-miscible system maltitol-polyvinylpyrrolidone (PVP) was studied; see Scheme 1 for their structures. Maltitol is a sugar alcohol and well-characterized glass former. PVP is a common excipient in ASDs and in wet granulation.[18] X-ray photoelectron spectroscopy (XPS) was used to measure the surface concentration of PVP [14, 15,17] and its enrichment kinetics. We find that PVP has a strong tendency to enrich at the surface of maltitol and the tendency increases with its molecular weight. The rate of surface enrichment is controlled by the vertical diffusion rate of PVP to reach the surface layer and the extracted diffusion coefficients match reasonably well with those calculated from bulk viscosity and the Stokes-Einstein equation. To our knowledge, this is the first measurement of the kinetics of surface enrichment in an ultra-viscous glass-forming liquid.

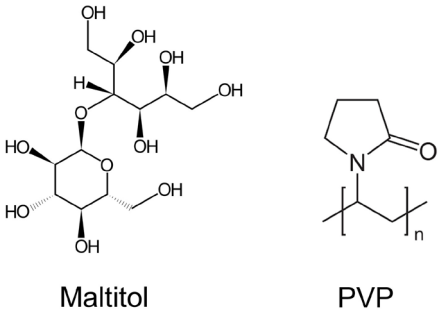

Scheme 1. Structures of maltitol and PVP.

Materials and Methods

Materials. Maltitol (98 %) was purchased from Sigma-Aldrich (St. Louis, MO) and purified by washing with ethanol and drying in an oven at 343-353 K. PVP K12 (M_w = 2000−3000 g/mol[19]), K15 (M_w = 8000 g/mol[19]), K30 (M_w = 44000−54000 g/mol[19]), and K90 (M_w = 1−2 M g/mol[19]) were obtained from BASF (Florham Park, NJ) and used as received. 1-Ethyl-2-pyrrolidone (98 %, "VP monomer") was purchased from Sigma-Aldrich (St. Louis, MO) and used as received.

Sample Preparation. Scheme 2 illustrates the steps of sample preparation and analysis. Maltitol-PVP mixtures were prepared by cryo-milling[20] (SPEX CertiPrep model 6750, Metuchen, NJ) using liquid nitrogen as coolant, followed by melting. Each mixture was 1 g and milled at 10 Hz for 5 cycles (5 min per cycle, 2 min cooldown between cycles). For a mixture in the 10−40 wt % PVP range, the ingredients were weighed and milled together. The 1 wt % mixture was obtained by diluting the 10 wt % mixture followed by cryo-milling. The 0.1 wt % mixture was obtained by diluting the 1 wt % mixture followed by cryo-milling.

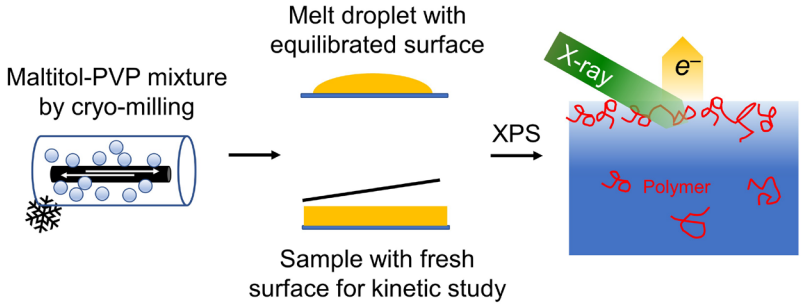

Scheme 2. Sample preparation and analysis.

Two kinds of open-surface samples were prepared. For the first kind, a 5 mg powder was melted at 430−440 K (the melting point of maltitol is 423 K) on a glass coverslip to form a droplet and

held for 30 min to degas. The sample was cooled to 298 K for XPS analysis. For the second kind, a 20 mg powder was melted and degassed as above. An aluminum foil was placed on the droplet to form a flat liquid film. The sample was cooled to 298 K and the foil was removed just before analysis. The sample of the first kind was used to study a well-equilibrated liquid surface and the sample of the second kind to study a freshly made surface and the kinetics of surface enrichment. In both cases, the sample thickness was approximately 20 μm, much thicker than the probe depth of XPS (~10 nm) and the thickness of the polymer-enriched layer at the liquid/air interface (~10 nm).[12,13] To assess potential contamination from the Al foil, the XPS spectrum of Al (2p orbital, near 75 eV[21]) was scanned and none was detected.

To measure the kinetics of surface enrichment, samples of the second kind (Al foil removed) were stored in a home-made mini-oven maintained at a target temperature (stable within ±0.5 K). The oven was placed in a sealed bag loaded with Drierite. The samples were periodically removed for analysis and returned to the mini-oven for further annealing until the next time point. In each experiment, a pure maltitol sample was included as control to check for cross-contamination by observing the PVP-specific nitrogen peak in the XPS spectrum. The pure maltitol control never developed a nitrogen peak during the experiment.

Differential Scanning Calorimetry (DSC). A TA Q2000 differential scanning calorimeter (New Castle, DE) was used to determine the miscibility between maltitol and PVP. Each sample of 5−10 mg was loaded in a crimped aluminum pan. The glass transition temperature T_g was measured as the onset during heating at 10 K/min after cooling at 10 K/min under 50 mL/min N_2 purge.

X-ray Photoelectron Spectroscopy (XPS). The experimental procedure and its validation has been described in Ref. 17. Briefly, the instrument was a Thermo Scientific X-ray Photoelectron Spectrometer (Waltham, MA) with an Al Kα (1486.6 eV) source. The measurements were performed in vacuum (10^{-5} Pa) at 297 K. An electron flood gun was used to neutralize the surface charge for the non-conductive samples. The X-ray spot size was 400 μm. Two positions in each sample were randomly chosen for measurements. A survey for all possible elements was performed at 1 eV step and passing energy of 200 eV. High-resolution scans for quantitative measurements of elements of interest were performed at 0.1 eV step and passing energy of 50 eV. XPS spectra were analyzed using the Thermo Scientific Avantage Data System. Peak positions were calibrated against the C 1s peak at 285.0 eV. The baseline for integration was obtained using a smart baseline function in the Avantage Data System. Based on the previous validation against 10 pure compounds, the error of the method was 5 % in atomic concentration.[17]

Results and Discussion

Polymer-host Miscibility. We established by DSC that PVP is miscible with maltitol in the bulk in the concentration range investigated (0−10 wt %). For this purpose, maltitol's glass transition temperature (T_g) was measured as a function of polymer concentration.[22] Figure 1 shows that with increasing PVP concentration, T_g increases up to 40 wt % PVP (using PVP K12 as an example). Since PVP K12 has higher T_g (375 K) than maltitol (318 K), this increase is expected and indicates that the two components are miscible at least up to 20 wt %. The miscibility of PVP with maltitol is consistent with its miscibility with other polyalcohols.[23]

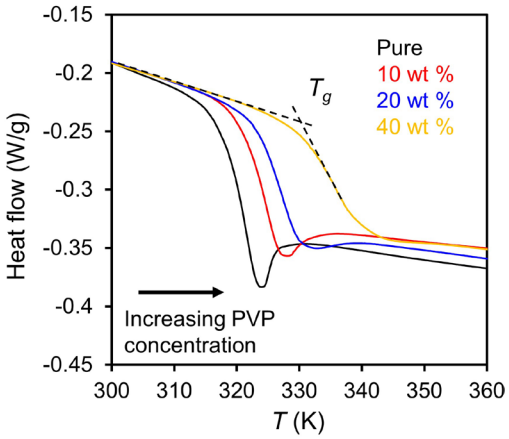

Figure 1. DSC traces showing the glass transition in maltitol doped with PVP K12. The increase of T_g with PVP concentration indicates that maltitol and PVP are miscible at least up to 20 wt %.

Surface Enrichment of PVP in Amorphous Maltitol. Figure 2 illustrates our measurement by XPS of the surface concentration of PVP in amorphous maltitol. Figure 2a shows the survey spectra for pure maltitol and maltitol doped with PVP K12 at different concentration. The peaks labeled C, O, and N correspond to the element carbon (C 1s, 285 eV), oxygen (O 1s, 533 eV), and nitrogen (N 1s, 399 eV); the area of each peak is proportional to the surface atomic concentration of the corresponding element. These samples have been annealed for long times (see below) so that the surface composition has equilibrated. The nitrogen peak, unique to PVP (Scheme 1), is used to measure the PVP concentration. The pure maltitol shows only the C and O peaks, at a ratio of 1.12 ± 0.03 (n = 9), in agreement with the theoretical value based on its molecular formula, 1.09. The PVP K12 doped maltitol (0.1−10 wt %) all show a N peak, see Figure 2b, indicating its presence in the surface layer. The N peak is detected even at the lowest bulk concentration tested (0.1 wt %) and increases with increasing PVP concentration. In Figure 2b, the intensity of each N peak has been normalized by the intensity of the O peak so that the peak area is proportional to the N/O ratio at the surface.

Eq. 1 is used to calculate the surface concentration of PVP:

$$w_p = \frac{\frac{11k}{M_0}}{\frac{11k}{M_0}+\frac{1-k}{M_p}} \qquad (1)$$

where w_P is the weight fraction of the polymer, M_p is the molecular weight of the monomer, M_0 is the molecular weight of maltitol, and k is the measured N/O atomic ratio. This equation assumes independent responses of atoms in the region probed by the X-ray.

Figure 2c shows the calculated surface concentration of PVP K12 in amorphous maltitol as a function of its bulk concentration. The curve indicates the condition of equal concentrations at the surface and in the bulk. We find that the polymer's surface concentration is significant higher than its bulk value. At 0.1 wt % bulk concentration, the surface concentration is 17 wt %, corresponding to a surface-enrichment factor of 170. The surface concentration of PVP increases as its bulk concentration increases, and the increase is approximately linear on the logarithm of the bulk concentration. A similar relation has been reported for the surface enrichment of a polymer solution.[10, 24]

For a binary solution, the component with lower surface tension is expected to enrich in the liquid/vapor interface and thus lower the overall surface energy.[10, 15] The Prigogine-Maréchal model provides a quantitative model of this effect building on the Flory-Huggins model of polymer-solvent interactions.[10, 24] As Scheme 1 shows, maltitol is a polyol with many polar hydroxyl groups and PVP is less polar and expected to have a lower surface energy than maltitol. As a result, we expect PVP to enrich on the surface of amorphous maltitol. (At present, the surface energies of maltitol and PVP are unknown, but we can make a rough assessment based on their analogs. Glycerol, a smaller polyol than maltitol, has a surface energy of 63.4 mN/m at 293 K.[25] The dimer of vinyl pyrrolidone ("VP dimer") has a surface tension of 39.8 mN/m at 299 K.[15] Using these values as a guide, we expect PVP to have lower surface tension than maltitol and be the component of surface enrichment.)

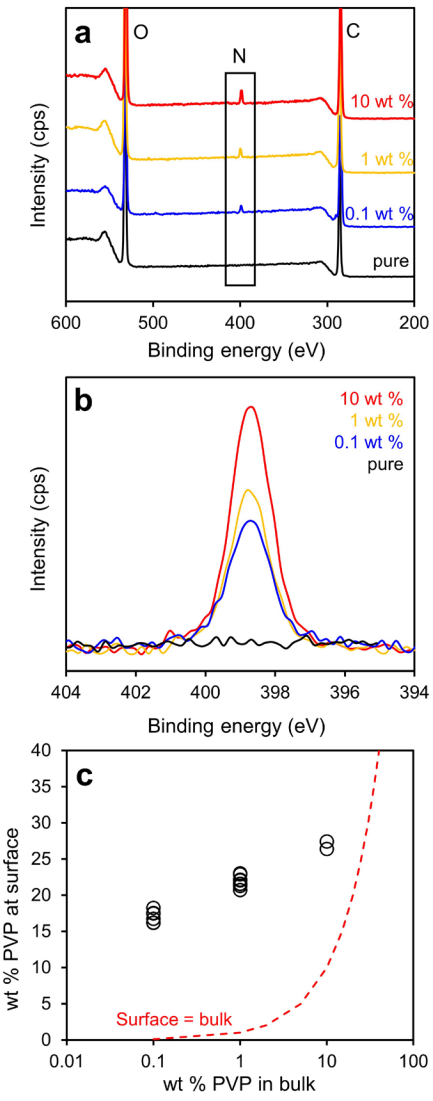

Figure 2. (a) XPS survey scans of maltitol containing PVP K12. REDUCE/MOVE THE WT% LABELS SO THEY DON'T TOUCH THE AXIS OR DATA. (b) High-resolution scans of the N peak. The intensity is normalized by the O peak so the peak area is proportional to the N/O ratio. (c) Surface concentration of PVP K12 vs bulk concentration.

Figure 3 shows how the surface concentration of PVP in amorphous maltitol changes with its molecular weight (MW), while the bulk concentration was kept constant at 1 wt %. As the MW increases, the surface concentration increases slightly. Note that the "VP monomer" shows very little surface enrichment. The surface energy of a polymer is expected to increase with its MW.[26] Thus, the trend observed is not driven by surface energy; otherwise a decrease of surface concentration is expected with increasing MW. A possible cause for the observed effect is the reduced entropy penalty of surface segregation for larger molecules from a small-molecule host (in the Flory-Huggins theory, the entropy of mixing of a small molecule with a polymer decreases as the polymer's MW increases).[10, 24]

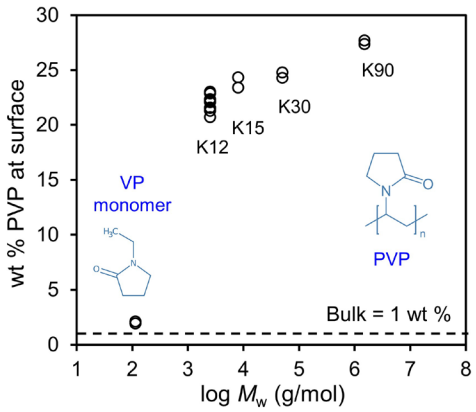

Figure 3. Surface concentration of PVP vs its molecular weight at a constant bulk concentration (1 wt %).

Kinetics of Polymer Surface Enrichment. Figure 4a shows the evolution of the N peak in the XPS spectrum as a freshly prepared surface of PVP K12-doped maltitol is annealed. The bulk concentration of the polymer is 1 wt % and the annealing temperature is 328 K (T_g + 10 K). At time zero, no nitrogen peak was detected; with annealing, the N peak grew. This indicates an increase of the polymer concentration at the surface. Figure 4b shows the surface concentration of PVP as a function of annealing time. For the sample in Figure 4a (red symbols), the surface concentration of PVP increases from undetectable at time zero to 18 wt % after 7 days. The increase was fast initially and slowed down over time.

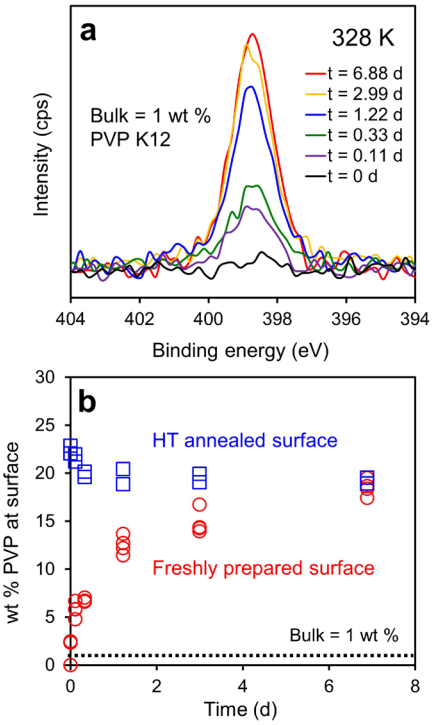

Figure 4. (a) The N peak of a fresh surface of maltitol containing 1 wt % PVP K12 at 328 K (T_g + 10 K). The intensity has been normalized by the O peak so each peak area is proportional to the surface N/O value. (b) Surface concentration of PVP vs annealing time for the sample in (a) and for an open-surface sample of the same bulk composition that had been equilibrated at high temperature before annealing at 328 K.

For comparison, Figure 4b also shows the data for an open-surface sample of the same bulk composition that had been equilibrated at a high temperature and cooled to 328 K. Initially, this sample had a high surface concentration of PVP (22 wt %) because of equilibration at high temperature. During storage at 328 K, the surface concentration decreased slightly and stabilized at 19 wt %. This concentration agrees within experimental error with the value reached by the fresh-surface sample in Figure 4a that had been annealed only at 328 K. These two samples

had different histories and approached the equilibrium state from two opposite directions. The fact that they approached the same equilibrium state indicates that the final concentration reached is the true equilibrium for surface concentration.

We interpret the results in Figure 4 as follows. For the freshly made open-surface sample in Figure 4a, the initial surface concentration of PVP was at the bulk value (1 wt %), which is below the detection limit of XPS. With annealing at 328 K, PVP's surface concentration increased and eventually plateaued. For the sample whose surface had been equilibrated at a high temperature, the initial PVP surface concentration was high and during annealing at 328 K, only a small adjustment of surface concentration took place, reflecting the temperature effect on equilibrium surface concentration. For both samples, the evolution of the surface concentration provided information on the kinetics of surface enrichment.

Figure 5a shows the kinetics of surface enrichment of PVP at different temperatures in maltitol containing 1 wt % PVP K12. The evolution is faster at higher temperature, and in the temperature range investigated, the rate of surface enrichment spans 4 orders of magnitude. In Figure 5a, the data at different temperatures are plotted against the logarithm of time, and in this format, appear parallel to each other. This suggests that they can be collapsed to a master curve by multiplying the measurement time at each temperature by a factor a_T. Figure 5b shows that this is indeed the case. This is the so-called time-temperature-superposition (TTS) behavior.[27] According to TTS, if the surface concentration evolves as $f(t)$ at one temperature, the evolution is given by $f(a_T\, t)$ at a different temperature. The factor a_T indicates the relative rates of surface enrichment at different

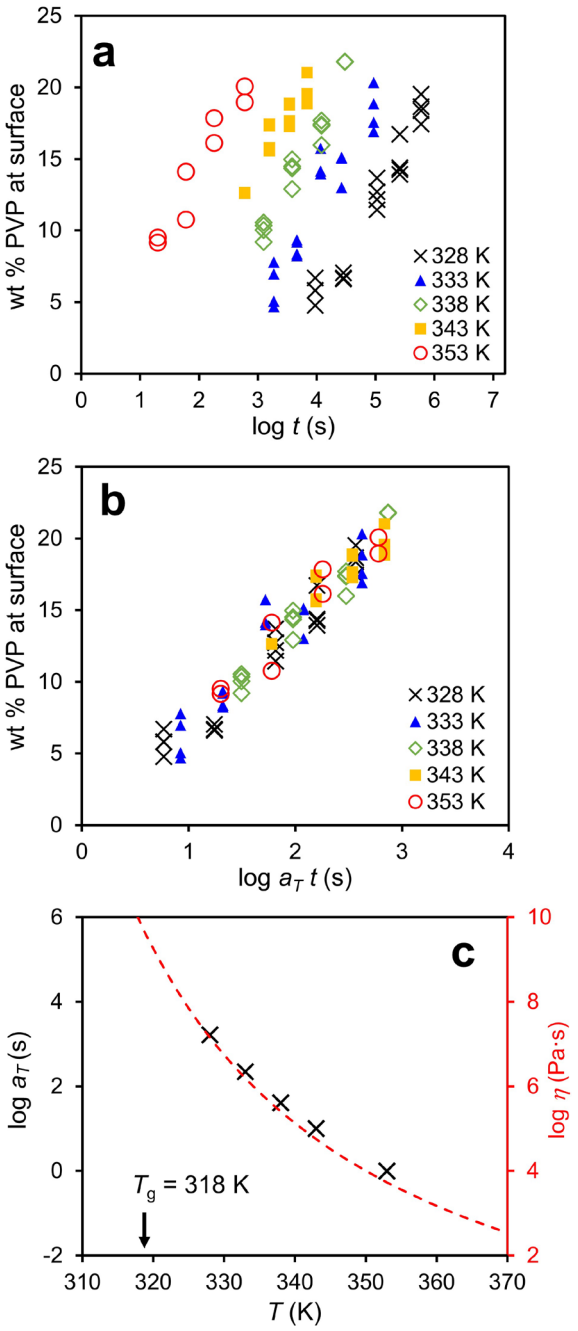

Figure 5. (a) Evolution of PVP surface concentration at different temperatures for maltitol containing 1 wt % PVP K12. (b) Master curve formed by laterally shifting the data in (a). a_T is the shift factor. (c) Temperature dependence of the shift factor a_T. The curve is the viscosity of maltitol plotted using the second y axis.

temperatures. In forming the master curve in Figure 5b, a_T is set to 1 at 353 K.

Figure 5c shows the shift factor a_T as a function of temperature. We find that a_T increases with cooling and the temperature dependence closely follows that of maltitol's viscosity,[28] plotted using the second y axis. This result indicates that the kinetics of PVP surface enrichment is strongly correlated with the bulk dynamics of the host medium. Surface enrichment requires the diffusion of polymer chains from the bulk to the surface region and according to the Stokes-Einstein relation, the diffusion rate of dilute polymer chains is inversely proportional to the solvent viscosity.[29] This is precisely the observed relation in Figure 5c. Later we will quantitatively compare the diffusion coefficients calculated from the surface-enrichment kinetics and the Stokes-Einstein relation.

Building on the idea above, we use a simple diffusion model to fit the observed kinetics of surface enrichment. We imagine an adsorption process where polymer molecules diffuse from a half-space of uniform initial concentration to the free surface, saturating at the equilibrium surface concentration (Figure 6a). At equilibrium, the concentration profile of the polymer is expected to have a characteristic length on the order of 10 nm.[12,13] We assume that XPS probes the molecules within a surface layer of thickness $L \sim 10$ nm.[17] For this process, the amount observed in the probed layer is given by:

$$M(t) = A\left[1 - \mathrm{erf}\left(\frac{L}{\sqrt{4Dt}}\right)\right] + M(0) \qquad (2)$$

where $M(0)$ is the amount present at time zero, $M(t)$ is the amount at time t, D is the diffusion coefficient, and A is the increase of the amount detected at equilibrium. This equation is analogous to that for the diffusion of a thin, high-concentration surface layer into a uniform half-space and can be derived in the same way with a change of sign and boundary condition.[30]

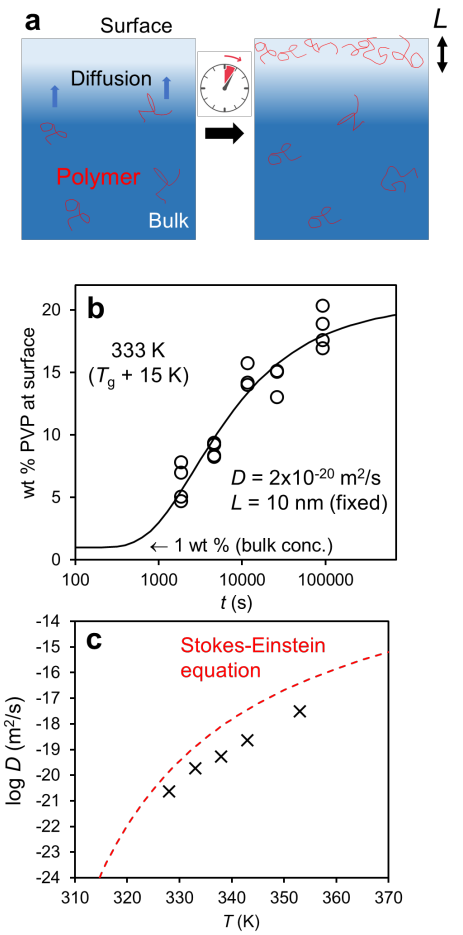

Figure 6. (a) Illustration of a diffusion-controlled surface enrichment process. (b) An example of fitting the observed enrichment kinetics to eq. 3. From the fit we obtain the diffusion coefficient D for the surface enrichment of PVP in maltitol. (c) D plotted against temperature. The curve is the bulk diffusion coefficient of dilute PVP in maltitol calculated from viscosity and the Stokes-Einstein equation.

Dividing eq. 2 by L (probe depth) and the probe area, we obtain:

$$c(t) = \Delta c \left[1 - \mathrm{erf}\left(\frac{L}{\sqrt{4Dt}}\right)\right] + c(0) \quad (3)$$

where $c(0)$ is the initial concentration, $c(t)$ is the concentration at time t, and Δc is the change of concentration at equilibrium.

Figure 6b illustrates a typical fitting result. In this sample, T = 333 K, c (0) = 1 wt % (bulk concentration), and L is assumed to be 10 nm (probe depth of XPS). The fit is reasonably good and from it we obtain the diffusion coefficient for the surface enrichment of PVP K12 in maltitol: log D (m^2/s) = -19.7. This and other values of D are plotted in Figure 6c against temperature. The curve in Figure 6c is the bulk diffusion coefficient of dilute PVP in maltitol calculated from the Stokes-Einstein equation:

$$D = k_B T/(6\pi\eta R_g) \quad (4)$$

where η is maltitol's viscosity[28] and R_g is the radius of gyration of the polymer. For PVP K12, R_g = 1.23 nm in an aqueous solution according to quasi-elastic light scattering[31] and we assume the same value holds for maltitol as solvent. Figure 6c shows a reasonable agreement between the polymer diffusion coefficients for surface enrichment and bulk diffusion (from eq. 4). The D values for surface enrichment appear to be smaller (by a factor of ~10), but the difference could arise from the errors in R_g and the assumed probe depth of XPS. In fact, it seems more surprising that the diffusion rates in the surface region are so *similar* to those in the bulk, a point to be discussed below.

Vertical and Lateral Diffusion in the Surface Layer. Molecules in the surface region of a liquid have different structure and dynamics from those in the bulk. In a molecular glass, surface diffusion is often vastly faster than bulk diffusion.[5] For a multicomponent liquid, the surface composition generally differs from the bulk composition. Given these effects, it might come as a surprise that PVP diffusion in the near-surface region of maltitol has about the same rate as that in the bulk (Figure 6c). Several factors could contribute to this result. First, the diffusion measured in this work is the *vertical* migration of polymer chains toward the surface (Figure 6a), whereas the surface diffusion measured in the previous work (e.g., through the flattening of surface gratings)[5] is the *lateral* migration of molecules. These two rates need not be the same. For polystyrene, the vertical diffusion rate near the surface was measured using isotope-labeled layers and found to be slower than bulk diffusion.[32] Second, maltitol is a hydrogen-bonded liquid and its

lateral surface diffusion is substantially slower than that in non-associating van der Waals liquids.[33] This is a result of the robustness of hydrogen bonds: on going from the bulk to the surface, the number of hydrogen bonds per molecule does not change significantly, leaving the activation barrier for diffusion largely unchanged. Third, even for the lateral surface migration, a polymer may have much lower mobility than a small molecule. This is not only because a polymer is larger but also because it may penetrate deeper into the bulk where mobility is low.[34] This would anchor the polymer chains and limit their lateral center-of-mass migration. Together, these effects make the observed polymer diffusion rate for surface enrichment essentially the same as that for bulk diffusion.

Significance for ASD stability and performance. The key result of this work is that the polymer concentration at the surface of an ASD can deviate from its bulk concentration and the rate at which the surface concentration equilibrates is controlled by the rate of polymer diffusion through the host medium. It is important to note that throughout this process, the components remain miscible in the bulk and the concentration change occurs only in the surface layer. Because the surface is only a small portion of the overall material, the surface enrichment effect will not significantly alter the bulk concentration. We now consider the significance of our finding in the development of ASDs.

We first consider the timescale for the surface concentration to equilibrate after the creation of a fresh surface. Figure 7 shows the surface equilibration time of PVP K12 in maltitol as a function of temperature. We plot the time for the surface composition to reach the midpoint between the initial bulk concentration and the equilibrium surface concentration, $t_{1/2}$. The symbols are the measured data points (Figure 5a), ranging from minutes to one day. The curve is the viscosity of maltitol that has been scaled to coincide with the measured points. The good match between the data points and the scaled viscosity allows us to predict the surface equilibration time at lower temperatures. A decrease of temperature from the region of measurement would quickly slowdown the surface enrichment process. This is a consequence of the rapid rise of viscosity with cooling in a glass-forming molecular liquid. At T_g (318 K), $t_{1/2}$ is predicted to be one year. The result in Figure 7 pertains to PVP in the molecular weight (MW) grade K12 and a change of MW is expected to alter the polymer's diffusivity and its $t_{1/2}$ value. In the framework of the Stokes-Einstein relation (eq. 4), this effect can be estimated from the dependence of the polymer's R_g on MW. According to eq.

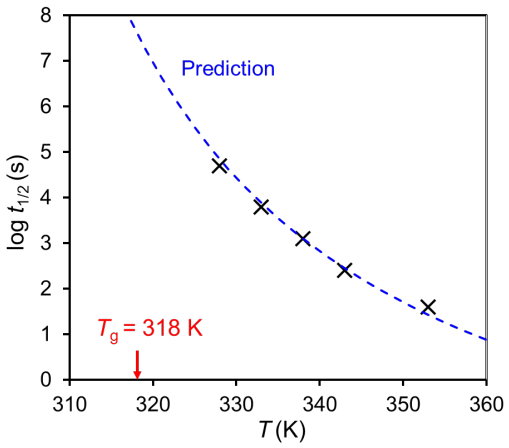

Figure 7. $t_{1/2}$ for the surface enrichment of PVP K12 in amorphous maltitol. $t_{1/2}$ is the time for the surface concentration to reach the halfway between the initial bulk value and the equilibrium surface value. The symbols are the measured data; the curve is the scaled viscosity.

4, $D \propto R_g^{-1}$ and $t_{1/2} \propto D^{-1} \propto R_g$. For PVP, changing the MW grade from K12 to K90 increases R_g by a factor of 15,[31] and is expected to decrease D and increase $t_{1/2}$ by the same factor.

The slow equilibration of a polymer's surface concentration in an amorphous system at low temperatures (near T_g or below) explains why a surface-deposited polymer nano-coating on an amorphous drug can persist for a long time, with little sign of migration into the bulk.[8] This enables the coating to suppress surface mobility and inhibit surface crystallization. The long-lasting coating has additional benefits of improving wetting and dissolution. Conversely, if fresh surfaces are created in an amorphous formulation by milling or fracture, the surface composition might not equilibrate immediately but would evolve slowly during storage. The evolution could be accelerated by heating above T_g and possibly by exposure to moisture. The effects discussed above pertain to the slow-diffusing polymers. For a high-mobility component in an ASD (e.g., a surfactant),[17] the rate of surface equilibration should be faster than that of a polymer. If a fresh surface is created in an ASD, the surfactant will likely migrate to the surface faster than the polymer, causing a local segregation of excipients.

Recently, Yao et al. reported that crystal nucleation is vastly enhanced at the liquid/vapor interface of D-arabitol relative to the bulk and selects a different polymorph [Yao, X., Liu, Q., Wang, B., Yu, J., Aristov, M. M., Shi, C., ... & Yu, L. Anisotropic Molecular Organization at a Liquid/Vapor Interface Promotes Crystal Nucleation with Polymorph Selection. Journal of the American Chemical Society. 2022, 144, 26, 11638–11645] They found that this process is inhibited by a PVP in trace amount because of the surface-enrichment effect. At a bulk concentration of 20 ppm, the surface concentration of PVP K30 is 15 % or 10^4 times higher, leading to significant inhibition of surface nucleation. This example illustrates a potentially significant effect of polymer surface enrichment on drug crystallization in an ASD. The magnitude of the effect will vary system to system, depending on the surface concentration of the polymer, on the surface-to-volume ratio, and on whether crystal nucleation or growth is considered.

Conclusions

Using XPS we have measured the kinetics of surface enrichment of a polymer in a glass-forming molecular liquid for the first time. We observe a strong tendency for the polymer PVP to enrich on the surface of amorphous maltitol and this occurs while the two components are fully miscible in the bulk. The rate of surface enrichment is controlled by the diffusion of the polymer from the bulk to the surface. The enrichment kinetics at different temperatures show time-temperature superposition (TTS) and the multiplicative factors have the same temperature dependence as the bulk viscosity of the host medium. Fitting the enrichment kinetics as diffusion-controlled adsorption yielded diffusion coefficients in reasonable agreement with those calculated from the Stokes-Einstein relation.

Our results are relevant for understating and developing amorphous materials. An amorphous material generally contains multiple components and generally has free surfaces. The free surfaces may be present in the as-prepared materials or created by grinding, fracture, and tableting. This and other studies[12-17] have shown that the surface composition of an amorphous material can be vastly different from its bulk composition even though the components are fully miscible in the bulk. This means that the properties of the material in the surface region are very different from those in the bulk region and the overall performance of the material will depend on the surface-to-volume ratio. This work has further shown that if a fresh surface is created in an amorphous material, the surface composition will evolve over time, controlled by the diffusion rate of the surface-migrating component. For the system of this study, the vertical migration rate of the polymer to the surface is reasonably well represented by its bulk diffusion rate (Figure 6c). This conclusion, if general, allows prediction of the surface-enrichment kinetics from the bulk mobility. At high temperatures, the surface composition equilibrates quickly, but if a fresh surface is created in the glassy state, the process can be slow and be highly sensitive to storage temperature, environmental moisture, and the nature of the diffusing species. This can in turn influence the stability, wettability, and dissolution of the material.

Acknowledgements

We thank BMS for supporting this work and the NSF-supported University of Wisconsin Materials Research Science and Engineering Center (DMR-1720415) for partial support and the use of its characterization facility.

References

(1) Ediger, M. D.; de Pablo, J.; Yu, L. Anisotropic vapor-deposited glasses: hybrid organic solids. *Accounts of chemical research* **2019**, *52* (2), 407-414.
(2) Yu, L. Amorphous pharmaceutical solids: preparation, characterization and stabilization. *Advanced drug delivery reviews* **2001**, *48* (1), 27-42.
(3) Ghebremeskel, A. N.; Vemavarapu, C.; Lodaya, M. Use of surfactants as plasticizers in preparing solid dispersions of poorly soluble API: selection of polymer–surfactant combinations using solubility parameters and testing the processability. *International journal of pharmaceutics* **2007**, *328* (2), 119-129.
(4) Van den Mooter, G. The use of amorphous solid dispersions: A formulation strategy to overcome poor solubility and dissolution rate. *Drug Discovery Today: Technologies* **2012**, *9* (2), e79-e85.
(5) Yu, L. Surface mobility of molecular glasses and its importance in physical stability. *Advanced drug delivery reviews* **2016**, *100*, 3-9.
(6) Hasebe, M.; Musumeci, D.; Powell, C. T.; Cai, T.; Gunn, E.; Zhu, L.; Yu, L. Fast surface crystal growth on molecular glasses and its termination by the onset of fluidity. *The Journal of Physical Chemistry B* **2014**, *118* (27), 7638-7646.

(7) Powell, C. T.; Xi, H.; Sun, Y.; Gunn, E.; Chen, Y.; Ediger, M.; Yu, L. Fast crystal growth in o-terphenyl glasses: a possible role for fracture and surface mobility. *The Journal of Physical Chemistry B* **2015**, *119* (31), 10124-10130.
(8) Li, Y.; Yu, J.; Hu, S.; Chen, Z.; Sacchetti, M.; Sun, C. C.; Yu, L. Polymer nanocoating of amorphous drugs for improving stability, dissolution, powder flow, and tabletability: The case of chitosan-coated indomethacin. *Molecular pharmaceutics* **2019**, *16* (3), 1305-1311.
(9) Wu, T.; Sun, Y.; Li, N.; de Villiers, M. M.; Yu, L. Inhibiting surface crystallization of amorphous indomethacin by nanocoating. *Langmuir* **2007**, *23* (9), 5148-5153. Teerakapibal, R.; Gui, Y.; Yu, L. Gelatin nano-coating for inhibiting surface crystallization of amorphous drugs. *Pharmaceutical research* **2018**, *35* (1), 1-7.
(10) Siow, K.; Patterson, D. Surface thermodynamics of polymer solutions. *The Journal of Physical Chemistry* **1973**, *77* (3), 356-365.
(11) De Gennes, P. d. Polymer solutions near an interface. Adsorption and depletion layers. *Macromolecules* **1981**, *14* (6), 1637-1644.
(12) Bloch, J.; Sansone, M.; Rondelez, F.; Peiffer, D.; Pincus, P.; Kim, M.-W.; Eisenberger, P. Concentration profile of a dissolved polymer near the air-liquid interface: X-ray fluorescence study. *Physical review letters* **1985**, *54* (10), 1039.
(13) Lee, L.; Guiselin, O.; Lapp, A.; Farnoux, B.; Penfold, J. Direct measurements of polymer depletion layers by neutron reflectivity. *Physical review letters* **1991**, *67* (20), 2838.
(14) Kim, E. H.-J.; Chen, X. D.; Pearce, D. Surface composition of industrial spray-dried milk powders. 1. Development of surface composition during manufacture. *Journal of Food Engineering* **2009**, *94* (2), 163-168.
(15) Chen, Z.; Yang, K.; Huang, C.; Zhu, A.; Yu, L.; Qian, F. Surface enrichment and depletion of the active ingredient in spray dried amorphous solid dispersions. *Pharmaceutical Research* **2018**, *35* (2), 38.
(16) Chen, Y.; Chen, H.; Wang, S.; Liu, C.; Qian, F. A single hydrogen to fluorine substitution reverses the trend of surface composition enrichment of sorafenib amorphous solid dispersion upon moisture exposure. *Pharmaceutical Research* **2019**, *36* (7), 1-12.
(17) Yu, J.; Li, Y.; Yao, X.; Que, C.; Huang, L.; Hui, H.-W.; Gong, Y.; Qian, F.; Yu, L. Surface Enrichment of Surfactants in Amorphous Drugs: An X-ray Photoelectron Spectroscopy Study. *Molecular Pharmaceutics* **2022**, *19* (2), 654-660.
(18) Wyttenbach, N.; Kuentz, M. Glass-forming ability of compounds in marketed amorphous drug products. *European Journal of Pharmaceutics and Biopharmaceutics* **2017**, *112*, 204-208.
(19) Huang, C.; Powell, C. T.; Sun, Y.; Cai, T.; Yu, L. Effect of low-concentration polymers on crystal growth in molecular glasses: a controlling role for polymer segmental mobility relative to host dynamics. *The Journal of Physical Chemistry B* **2017**, *121* (8), 1963-1971.
(20) Tao, J.; Sun, Y.; Zhang, G. G.; Yu, L. Solubility of small-molecule crystals in polymers: D-mannitol in PVP, indomethacin in PVP/VA, and nifedipine in PVP/VA. *Pharmaceutical research* **2009**, *26* (4), 855-864.
(21) Chastain, J.; King Jr, R. C. Handbook of X-ray photoelectron spectroscopy. *Perkin-Elmer, USA* **1992**, 261.
(22) Sun, Y.; Tao, J.; Zhang, G. G.; Yu, L. Solubilities of crystalline drugs in polymers: an improved analytical method and comparison of solubilities of indomethacin and nifedipine in PVP, PVP/VA, and PVAc. *Journal of pharmaceutical sciences* **2010**, *99* (9), 4023-4031.
(23) Yao, X.; Huang, C.; Benson, E. G.; Shi, C.; Zhang, G. G.; Yu, L. Effect of polymers on crystallization in glass-forming molecular liquids: equal suppression of nucleation and growth and master curve for prediction. *Crystal Growth & Design* **2019**, *20* (1), 237-244.
(24) Prigogine, I.; Marechal, J. The influence of differences in molecular size on the surface tension of solutions. IV. *Journal of colloid science* **1952**, *7* (2), 122-127.

(25) Association, G. P. *Physical properties of glycerine and its solutions*; Glycerine Producers' Association, 1963.
(26) Wu, S. Surface and interfacial tensions of polymer melts. II. Poly (methyl methacrylate), poly (n-butyl methacrylate), and polystyrene. *The Journal of Physical Chemistry* **1970**, *74* (3), 632-638.
(27) Simon, S.; Sobieski, J.; Plazek, D. Volume and enthalpy recovery of polystyrene. *Polymer* **2001**, *42* (6), 2555-2567.
(28) Nakheli, A.; Eljazouli, A.; Elmorabit, M.; Ballouki, E.; Fornazero, J.; Huck, J. La viscosité du maltitol. *Journal of Physics: Condensed Matter* **1999**, *11* (41), 7977.
(29) Stadelmaier, D.; Kohler, W. Thermal diffusion of dilute polymer solutions: the role of chain flexibility and the effective segment size. *Macromolecules* **2009**, *42* (22), 9147-9152.
(30) Helfferich, F. A note on Crank's correspondence principle in diffusion with a variable diffusion coefficient. *Journal of Polymer Science Part B: Polymer Letters* **1963**, *1* (2), 87-91. Crank, J. *The mathematics of diffusion*; Oxford university press, 1979.
(31) Armstrong, J. K.; Wenby, R. B.; Meiselman, H. J.; Fisher, T. C. The hydrodynamic radii of macromolecules and their effect on red blood cell aggregation. *Biophysical journal* **2004**, *87* (6), 4259-4270.
(32) Pu, Y.; Rafailovich, M.; Sokolov, J.; Gersappe, D.; Peterson, T.; Wu, W.-L.; Schwarz, S. Mobility of polymer chains confined at a free surface. *Physical Review Letters* **2001**, *87* (20), 206101.
(33) Chen, Y.; Zhang, W.; Yu, L. Hydrogen bonding slows down surface diffusion of molecular glasses. *The Journal of Physical Chemistry B* **2016**, *120* (32), 8007-8015.
(34) Li, Y.; Zhang, W.; Bishop, C.; Huang, C.; Ediger, M.; Yu, L. Surface diffusion in glasses of rod-like molecules posaconazole and itraconazole: Effect of interfacial molecular alignment and bulk penetration. *Soft Matter* **2020**, *16* (21), 5062-5070.